

A Windmill-Shaped Discotic Columnar Liquid Crystal with Fast Ambipolar Charge Carrier Transport

XuYing Liu,[†] Takayuki Usui,^{†,‡} and JunIchi Hanna^{*,†,‡}

[†]Imaging Science and Engineering Laboratory, Tokyo Institute of Technology, 4259 Nagatsuta Midori-ku, Yokohama 226-8503, Japan

[‡]CREST, Japan Science and Technology Agency, 4259 Nagatsuta Midori-ku, Yokohama 226-8503, Japan

Supporting Information

Various design concepts have been proposed to arrange the molecular organization for better charge carrier transport properties, including utilization of various molecular assemblies¹ and liquid crystalline mesophases.² Above all, the columnar mesophases in discotic liquid crystals (DLCs) have been extensively studied in various molecules such as triphenylenes,³ phthalocyanines,⁴ and hexabenzocoronenes,⁵ in which disc-shaped molecules self-organizing into one-dimensional molecular columns as conduction channels are expected to show high mobility. In fact, the existence of translational and rotational molecular motions⁶ originated from electrostatic repulsion and fluctuating flexible side chains (the length always over 10 Å)⁷ (Figure 1a) tends to decrease the transfer integral, which explains the reason for relatively low charge carrier mobility ranging from 10⁻⁴ to 10⁻² cm² V⁻¹ s⁻¹ in columnar mesophases of conventional discotic molecules.⁸

In order to achieve higher charge carrier mobility over 10⁻¹ cm² V⁻¹ s⁻¹ (close to that of a-Si) in discotic columnar phases, one may consider how to suppress the molecular motions in

the columns. Previously, complementary approaches have been carried out, including polytopic interaction (CPI)-based discotics⁹ and gelled DLC molecules with hydrogen-bonded fibrous aggregates,¹⁰ in addition to shortening intercolumnar space directly by shorter side chains,^{3,11} which consequently resulted in higher charge carrier mobility up to 10⁻² cm² V⁻² s⁻¹. Recently, it was found that DLC carbazole macrocycles with inward side chains were able to give rise to strong intercolumnar coupling due to minimized intercolumnar space, which could form a three-dimensional pathway for carriers to avoid traps, eventually leading to mobility of 10⁻¹ cm² V⁻² s⁻¹ simulated using the kinetic Monte Carlo method.¹²

It is noteworthy that to form homeotropic columnar mesophase requires the incorporation of complex peripheral side chains into dislike cores, which actually should be responsible for defects and molecular misorientation. Herein, we propose a new molecular design, i.e., the windmill-shaped molecule based on a disc-like truxene core (Figure 1b), in which a short monoside chain is adopted at a bay position to induce the homeotropic columnar mesophase. Generally, the shorter side chain forms a much narrower intermolecular distance between adjacent columns, contributing to suppressing the molecular motions (translational and rotational). Moreover, what's more important is to expose the peripheral phenyl ring, thus leading to less static defects along quasi one-dimensional columns, while forcing a face-to-face stacking of molecular cores is expected to maximize intermolecular couplings, thereby enhancing charge carrier transport within columns.

According to the present strategy, we designed truxene derivatives of 1,5,9-trialkyltruxene (Scheme 1). The implementation of this strategy began with the multigram-scale synthesis of hydroxyindanone **2** from the inexpensive dihydrocumarin **1** through a literature procedure.¹³ The intermediate **2** was triflated to produce **3** with *N,N*-bis(trifluoromethylsulfonyl)-phenylamine at room temperature at a high yield up to 70% prior to the alkylation via Suzuki coupling reaction. At last, intermolecular cyclocondensation reactions were performed under mild conditions by treating a synthetic block, **4**, with acid to afford the final truxenes of **Tru4** and **Tru6** at the yields of 63% and 52%, respectively, after purification by column chromatography. It is worth noting that this synthetic pathway for the truxene derivative actually is short and efficient, which

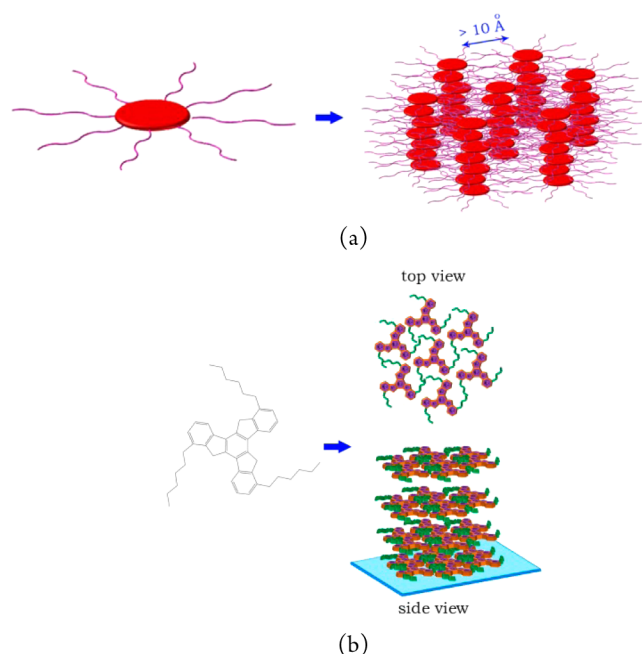
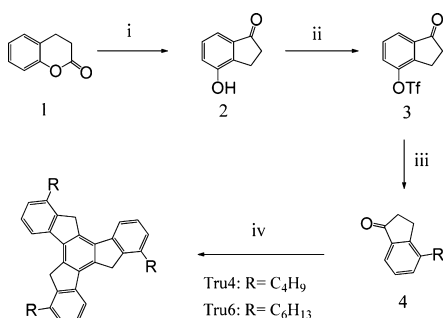


Figure 1. Schematic illustration of a conventional DLC peripherally substituted truxene (a) and a windmill-shaped DLC truxene (b) in hexagonal columnar mesophases.

Received: July 15, 2014

Revised: September 17, 2014

Published: September 18, 2014

Scheme 1. Synthetic Route for Windmill Shaped Truxene Derivatives^a

^ai, AlCl₃, NaCl, 200 °C; ii, *N,N*-bis(trifluoromethylsulfonyl)-phenylamine, Et₃N, DCM, 24 h; iii, alkyboronic acid, Pd(dppf)Cl₂, Ag₂O, K₂CO₃, THF; iv, HCl, HOAc, 120 °C.

might help to avoid contamination of chemical impurities that make it difficult to characterize charge carrier transport by time-of-flight experiments.

The phase transition behaviors of both truxenes were investigated by differential scanning calorimetry (DSC) and polarized optical microscope (POM). Compound **Tru4** did not show clear mesophase transition upon heating (Figure S1a, Supporting Information), only exhibiting one exothermic peak at 250 °C, while exhibiting a mesophase from 220 to 209 °C with a few dendritic textures observed in POM before crystallization upon cooling (Figure S2a, Supporting Information), and this irreversible phase transition is probably relative to the strong crystallinity of **Tru4**. Furthermore, the resulting mesophase was identified to be hexagonal columnar phase with homeotropic alignment. In the polycrystalline phase, a lot of cracks were observed (Figure S2b, Supporting Information). In contrast to **Tru4**, **Tru6** exhibited various thermal behaviors (Figure S1b, Supporting Information). The DSC plot indicates that two mesophases appeared in a temperature range from 127 to 175 °C in addition to the crystal phase below 127 °C and isotropic phase over 175 °C in the heating process, while upon cooling, the peak (11.36 J/g) at 127 °C is quite smaller than that (22.08 J/g) in the first heating process, which is usually identified to be the liquid crystal glass transition.¹⁴

Through observation of POM images of **Tru6**, its large dendritic textures up to several hundred micrometers (Figure 2a) clearly indicated the presence of a highly ordered hexagonal columnar phase in homeotropic alignment.¹⁵ Moreover, the dendritic textures turned to be leaf-like with large domains (Figure 2b) in the second liquid crystal phase, probably due to the appearance of a higher order structure, and finally this

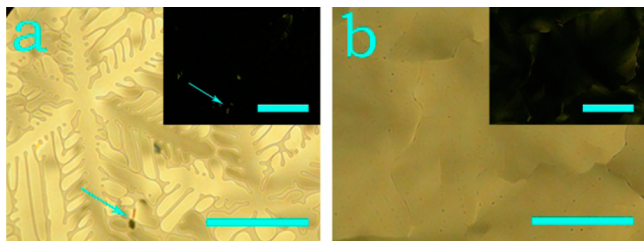


Figure 2. Normal and polarized optical microscope images of **Tru6** in different phases; a and b were taken without crossed polarizers, while the insets in a and b were with crossed polarizers. All scale bars represent 100 μm. The blue arrows point out defects.

texture was still observed at low temperatures, supporting a liquid crystal glass. When the sample stayed in ambient atmosphere overnight, it was found to crystallize and show clear birefringence in the whole visible region.

In order to investigate the microscopic molecular configuration in columnar phases, a study of variable-temperature XRD measurement was conducted in three phases of **Tru6**, i.e., the first mesophase at 160 °C, the second one at 140 °C, and the glass phase at 30 °C (Figure 3a). Upon cooling at 160 °C a

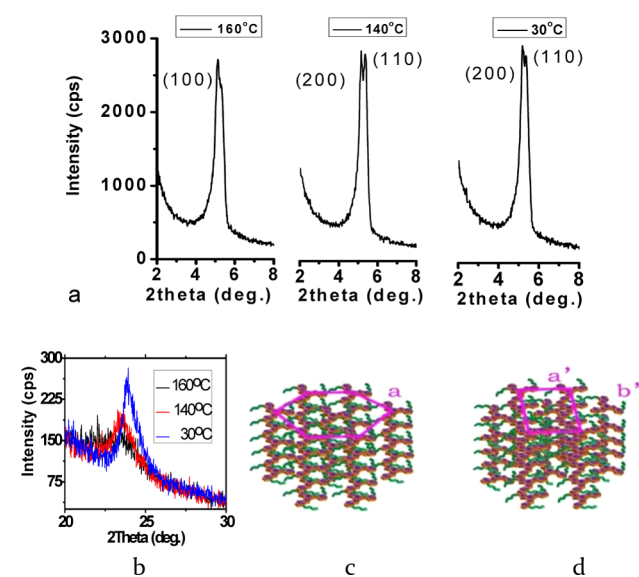


Figure 3. XRD patterns of **Tru6** in three phases, i.e., hexagonal columnar phase, rectangular columnar phase, and glass phase (a: small angle regions; b: wide angle regions), and illustration of columnar lattice (c: hexagonal columnar lattice and d: rectangular columnar phase). a, a', and b' represent lattice parameters.

peak appearing at 23.3° corresponds to the average core-to-core correlation of 3.80 Å, which is assigned to a highly ordered hexagonal columnar phase, combined with the intense low angle peak indexed to (100) that is attributed to a typical hexagonal unit cell with the parameter of $a = 19.2$ Å (Figure 3c). In particular, the molecular diameter of **Tru6** is calculated to be around 20 Å, which is a good agreement with the small lattice parameter. This indicates that **Tru6** molecules in mesophases tend to arrange tightly to compress intermolecular space, so that they sit in a restricted lattice. As expected, the minimum distance among adjacent columns was estimated to be less than 5 Å (core to core) as schematically illustrated in Figure 1b, which is quite narrow compared with that of peri-substituted DLC truxene (Figure 1a),^{11b,c} which is so close to a typical π - π interaction distance of 3.5 to 4 Å in a column.

Tru6 exhibited another columnar phase when cooled down to 144 °C. Obviously, it is an ordered mesophase because of the appearance of the peak (23.5°) at a wide angle region of the XRD pattern at 140 °C. At the low angle region of XRD pattern, the (100) face in the hexagonal lattice split into (200) and (110), which is typical for an ordered rectangular columnar phase (Col_{ro}) (Figure 3d). Indeed, the slight split supports that the phase transition from Col_{ho} phase to Col_{ro} just induced a trivial lattice variation. And also, the π - π interaction distance can be determined to be 3.75 Å, which is a little smaller than that in Col_{ho} phase, originated from a tilted molecular conformation in Col_{ro}. This typical Col_{ro} lattice remained in a

room temperature range, forming a glass phase, in which the peak at the wide angle region of the XRD pattern at 30 °C presented a right shift indicating a π - π interaction distance of 3.70 Å narrower than those in the two mesophases (Figure 3b).

To characterize charge carrier transport in densely packed columns formed in the windmill-shaped **Tru6**, we measured transient photocurrents by TOF experiments.¹⁶ Samples of **Tru6** were capillary-filled into a 9.3 μm thick liquid crystal cell with ITO electrodes at 180 °C in its isotropic phase. As shown in Figure 4a,b, well-defined nondispersive transient photo-

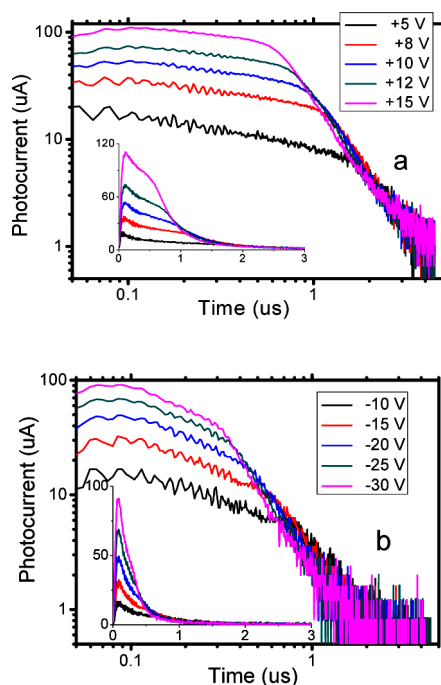


Figure 4. Typical transient photocurrents of **Tru6** at 165 °C in time-of-flight experiment; a: positive charge transport; b: negative charge transport.

currents for positive and negative charges were observed in the Col_{ho} phases of **Tru6** at 165 °C. Each photocurrent exhibited a clear shoulder, which indicates the transit time.

It is noted that mobility of hole and electron is almost constant irrespective of columnar and glassy phase, even if the phase structures are changed slightly as discussed above. In mesophases, the mobility depended on neither temperature nor electric field (Figure 5 and Figure S5, Supporting Information),

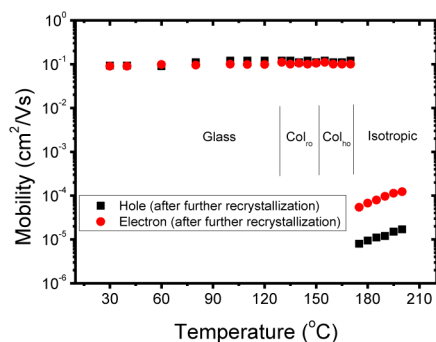


Figure 5. Temperature dependence of charge transport mobility in **Tru6**; the electric field was $1.1 \times 10^4 \text{ V cm}^{-1}$.

respectively, as is often reported in the liquid crystalline phases.¹⁹ This behavior can be well explained by a narrow distribution of the density of states less than 60 meV comparable to kT , where T is the temperature for TOF experiments²⁰ and is attributed to less disordered molecular alignment in the column and a small dipole moment of **Tru6**.

Author: This glass state was metastable and turned to be polycrystalline when the cell was kept at room temperature overnight. In the resulting polycrystalline film, non-dispersive photocurrent could be still observed (Figure S5, Supporting Information) and enables us to determine that charge carrier mobilities in the polycrystalline state are 0.2 and $0.17 \text{ cm}^2 \text{ V}^{-1} \text{ s}^{-1}$ for hole and electron, respectively, which are 2 orders of magnitude higher than those of DLC alkyl-substituted-benzocoronene derivatives.^{8d,21} They also hardly depended on neither temperature (Figure 5) nor electric field (Figure S6, Supporting Information) and were invariable for several weeks (Figure S7, Supporting Information). Polycrystalline **Tru4** also showed high ambipolar mobility around $0.3 \text{ cm}^2 \text{ V}^{-1} \text{ s}^{-1}$ (Figure S8, Supporting Information), which is the highest in all truxene derivatives.^{11b,c} It is well-known that the non-dispersive charge transport in polycrystalline thin films is rarely observed in nonliquid crystalline organic materials because defective grain boundaries cause deep trap states for charge carriers. Therefore, the fast charge transport in the truxenes is explained by preferential formation of grain boundaries along with the columns²² and/or possible charge transport among the columns thanks to the small intercolumnar space of 5 Å in the present polycrystalline films.

In summary, we synthesized novel windmill-shaped discotic liquid crystalline truxenes, i.e., 1,5,9-trialkyltruxene substituted with alkyl chains at bay-positions of truxene core. These truxenes showed highly ordered columnar phases with homeotropic alignment upon cooling, in which a very narrow intercolumnar space of 5 Å was estimated. The resulting columnar structure was quite stable and so densely packed that molecular motions in mesophases were thought to be confined. Interestingly, these DLC materials showed fast ambipolar carrier mobility over $0.1 \text{ cm}^2 \text{ V}^{-1} \text{ s}^{-1}$ in both columnar and crystalline phases in spite of a relatively small core size of truxene. These results suggest the windmill-shaped DLC molecules with short alkyl substituents at bay positions give densely packed columnar phases, which are advantageous over conventional DLC molecules substituted with peripheral side chains for fast charge carrier transport.³⁻⁵ This new molecular design strategy is expected to be applied in various π -conjugated systems, like phthalocyanine, tetrabenzoporphyrin, and trithiatruxene, which will make discotic liquid crystals more promising as organic semiconductors.

■ ASSOCIATED CONTENT

📄 Supporting Information

Details of synthesis and characterization of **Tru4** and **Tru6**, NMR, DSC, POM, and the results of transient photocurrents through time-of-flight technique. This material is available free of charge via the Internet at <http://pubs.acs.org>.

■ AUTHOR INFORMATION

Corresponding Author

*E-mail: hanna@isl.titech.ac.jp.

Notes

The authors declare no competing financial interest.

■ ACKNOWLEDGMENTS

We thank Prof. Dr. H. Iino, Ms. Y. Takayashiki, and Dr. A. Ohno for very useful discussion. This work was partly supported by CREST under the JST Strategic Basic Research Programs sponsored by Japan Science Agency.

■ REFERENCES

- (1) (a) Prasanthkumar, S.; Saeki, A.; Seki, S.; Ajayaghosh, A. *J. Am. Chem. Soc.* **2010**, *132*, 8866. (b) Lee, O. P.; Yiu, A. T.; Beaujuge, P. M.; Woo, C. H.; Holcombe, T. W.; Millstone, J. E.; Fréchet, J. M. *Adv. Mater.* **2011**, *23*, 5359. (c) Takacs, C. J.; Sun, Y.; Welch, G. C.; Perez, L. A.; Liu, X.; Wen, W.; Heeger, A. J. *J. Am. Chem. Soc.* **2012**, *134*, 16597.
- (2) (a) Kim, B. G.; Jeong, E. J.; Chung, J. W.; Seo, S.; Koo, B.; Kim, J. *Nat. Mater.* **2013**, *12*, 659. (b) Liu, X. Y.; Usui, T.; Hanna, J. I. *Chem.—Eur. J.* **2014**, DOI: 10.1002/chem.201403472. (c) Iino, H.; Hanna, J. I. *Adv. Mater.* **2011**, *23*, 1748. (d) Idé, J.; Méreau, R.; Ducasse, L.; Castet, F.; Bock, H.; Olivier, Y.; Cornil, J.; Beljonne, D.; Davino, G.; Roscioni, O. M.; Zannoni, L. M. *J. Am. Chem. Soc.* **2014**, *136*, 2911.
- (3) (a) Adam, D.; Schuhmacher, P.; Simmerer, J.; Häussling, L.; Siemensmeyer, K.; Etzbach, K. H.; Haarer, D. *Nature* **1994**, *371*, 141. (b) Osawa, T.; Kajitani, T.; Hashizume, D.; Ohsumi, H.; Sasaki, S.; Takata, M.; Aida, T. *Angew. Chem.* **2012**, *124*, 8114.
- (4) (a) Cook, M. J.; Daniel, M. F.; Harrison, K. J.; McKeown, N. B.; Thomson, A. J. *J. Chem. Soc., Chem. Comm.* **1987**, *14*, 1086. (b) Gbabode, G.; Dumont, N.; Quist, F.; Schweicher, G.; Moser, A.; Viville, P.; Geerts, Y. H. *Adv. Mater.* **2012**, *24*, 658.
- (5) (a) Schmidt-Mende, L.; Fechtenkötter, A.; Müllen, K.; Moons, E.; Friend, R. H.; MacKenzie, J. D. *Science* **2001**, *293*, 1119. (b) Van de Craats, A. M.; Warman, J. M.; Fechtenkötter, A.; Brand, J. D.; Harbison, M. A.; Müllen, K. *Adv. Mater.* **1999**, *11*, 1469.
- (6) (a) Lemaur, V.; Da Silva Filho, D. A.; Coropceanu, V.; Lehmann, M.; Geerts, Y.; Piris, J.; Cornil, J. *J. Am. Chem. Soc.* **2004**, *126*, 3271. (b) Haverkate, L. A.; Zbiri, M.; Johnson, M. R.; Deme, B.; Mulder, F. M.; Kearley, G. J. *J. Phys. Chem. B* **2011**, *115*, 13809. (c) Hansen, M. R.; Feng, X.; Macho, V.; Müllen, K.; Spiess, H. W.; Floudas, G. *Phys. Rev. Lett.* **2011**, *107*, 257801. (d) Haverkate, L. A.; Zbiri, M.; Johnson, M. R.; Deme, B.; Mulder, F. M.; Kearley, G. J. *J. Phys. Chem. B* **2012**, *116*, 3908.
- (7) (a) Elmahdy, M. M.; Dou, X.; Mondeshki, M.; Floudas, G.; Butt, H. J.; Spiess, H. W.; Müllen, K. *J. Am. Chem. Soc.* **2008**, *130*, 5311. (b) Mulder, F. M.; Stride, J.; Picken, S. J.; Kouwer, P. H.; De Haas, M. P.; Siebbeles, L. D.; Kearley, G. J. *J. Am. Chem. Soc.* **2003**, *125*, 3860.
- (8) (a) Bushby, R. J. *Mater. Chem.* **1999**, *9*, 2081. (b) Tatum, L. A.; Johnson, C. J.; Fernando, A. A.; Ruch, B. C.; Barakoti, K. K.; Alpuche-Aviles, M. A.; King, B. T. *Chem. Sci.* **2012**, *3*, 3261. (c) Jankowiak, A.; Pocięcha, D.; Szczytko, J.; Monobe, H.; Kaszyński, P. *J. Am. Chem. Soc.* **2012**, *134*, 2465. (d) Xiao, Q.; Sakurai, T.; Fukino, T.; Akaike, K.; Honsho, Y.; Saeki, A.; Aida, T. *J. Am. Chem. Soc.* **2013**, *135*, 18268.
- (9) Kreouzis, T.; Scott, K.; Donovan, K. J.; Boden, N.; Bushby, R. J.; Lozman, O. R.; Liu, Q. *Chem. Phys.* **2000**, *262*, 489.
- (10) Mizoshita, N.; Monobe, H.; Inoue, M.; Ukon, M.; Watanabe, T.; Shimizu, Y.; Kato, T. *Chem. Commun.* **2002**, *5*, 428.
- (11) (a) Simmerer, J.; Glösen, B.; Paulus, W.; Kettner, A.; Schuhmacher, P.; Adam, D.; Haarer, D. *Adv. Mater.* **1996**, *8*, 815. (b) Isoda, K.; Yasuda, T.; Kato, T. *Chem. Asian J.* **2009**, *4*, 1619. (c) Zhao, K. Q.; Chen, C.; Monobe, H.; Hu, P.; Wang, B. Q.; Shimizu, Y. *Chem. Commun.* **2011**, *47*, 6290.
- (12) (a) Vehoff, T.; Baumeier, B.; Andrienko, D. *J. Chem. Phys.* **2010**, *133*, 134901. (b) Jung, S. H.; Pisula, W.; Rouhanipour, A.; Räder, H. J.; Jacob, J.; Müllen, K. *Angew. Chem., Int. Ed.* **2006**, *45*, 4685.
- (13) Onyango, E. O.; Jacobi, P. A. *J. Org. Chem.* **2012**, *77*, 7411.
- (14) (a) Wu, J.; Usui, T.; Hanna, J. I. *J. Mater. Chem.* **2011**, *21*, 8045. (b) Lee, K. M.; Smith, M. L.; Koerner, H.; Tabiryan, N.; Vaia, R. A.; Bunning, T. J.; White, T. J. *Adv. Funct. Mater.* **2011**, *21*, 2913.
- (15) (a) Schweicher, G.; Gbabode, G.; Quist, F.; Debever, O.; Dumont, N.; Sergeyev, S.; Geerts, Y. H. *Chem. Mater.* **2009**, *21*, 5867.
- (b) Kajitani, T.; Suna, Y.; Kosaka, A.; Osawa, T.; Fujikawa, S.; Takata, M.; Aida, T. *J. Am. Chem. Soc.* **2013**, *135*, 14564.
- (16) Iino, H.; Hanna, J. I.; Haarer, D. *Phys. Rev. B* **2005**, *72*, 193203.
- (17) Iino, H.; Hanna, J. I.; Bushby, R. J.; Movaghar, B.; Whitaker, B. J.; Cook, M. J. *Appl. Phys. Lett.* **2005**, *87*, 132102.
- (18) Liu, X. Y.; Usui, T.; Iino, H.; Hanna, J. I. *J. Mater. Chem. C* **2013**, *1*, 8186.
- (19) (a) Pisula, W.; Tomovic, Z.; Simpson, C.; Kastler, M.; Pakula, T.; Müllen, K. *Chem. Mater.* **2005**, *17*, 4296. (b) Sergeyev, S.; Pisula, W.; Geerts, Y. H. *Chem. Soc. Rev.* **2007**, *36*, 1902. (c) Feng, X.; Marcon, V.; Pisula, W.; Hansen, M. R.; Kirkpatrick, J.; Grozema, F.; Andrienko, D.; Kremer, K.; Müllen, K. *Nat. Mater.* **2009**, *8*, 421.
- (20) Ohno, A.; Hanna, J. I. *Appl. Phys. Lett.* **2003**, *82*, 751.
- (21) Kastler, M.; Laquai, F.; Müllen, K.; Wegner, G. *Appl. Phys. Lett.* **2006**, *89*, 252103.
- (22) Iino, H.; Takayashiki, Y.; Hanna, J. I.; Bushby, R. J. *J. Appl. Phys.* **2005**, *44*, 1310.